Chapter 1
The Boom Clay

Contents

The Boom Formation, also called the Boom Clay, has been extensively investigated. The Boom Formation and the sedimentologically connected fine-grained and clayey deposits are used to define the Rupel Group (Vandenberghe, 2003). It is also mined in open pits as a raw material for the manufacturing of bricks and expanded clay products. Since the middle of the 1970’s, the Boom Clay has been studied as a candidate host rock for the geological disposal of long-lived radioactive waste in Belgium.

1.1 Location

The area where the Boom Clay is present corresponds approximately to the Campine basin of northern Belgium. The Boom Formation crops out in two areas, which form a belt from 5 to 15 km wide. The western outcrop is located to the north of the rivers Durme, Rupel and Dyle and the eastern outcrop is situated to the north of the Leuven-Tongeren line (Figure 1.1). The discontinuity of the outcrop area in the Hageland is due to the erosion of large parts of the sediments (or of the entire sediment at some places) by a system of channels, which was later filled by the Diestian Sands.

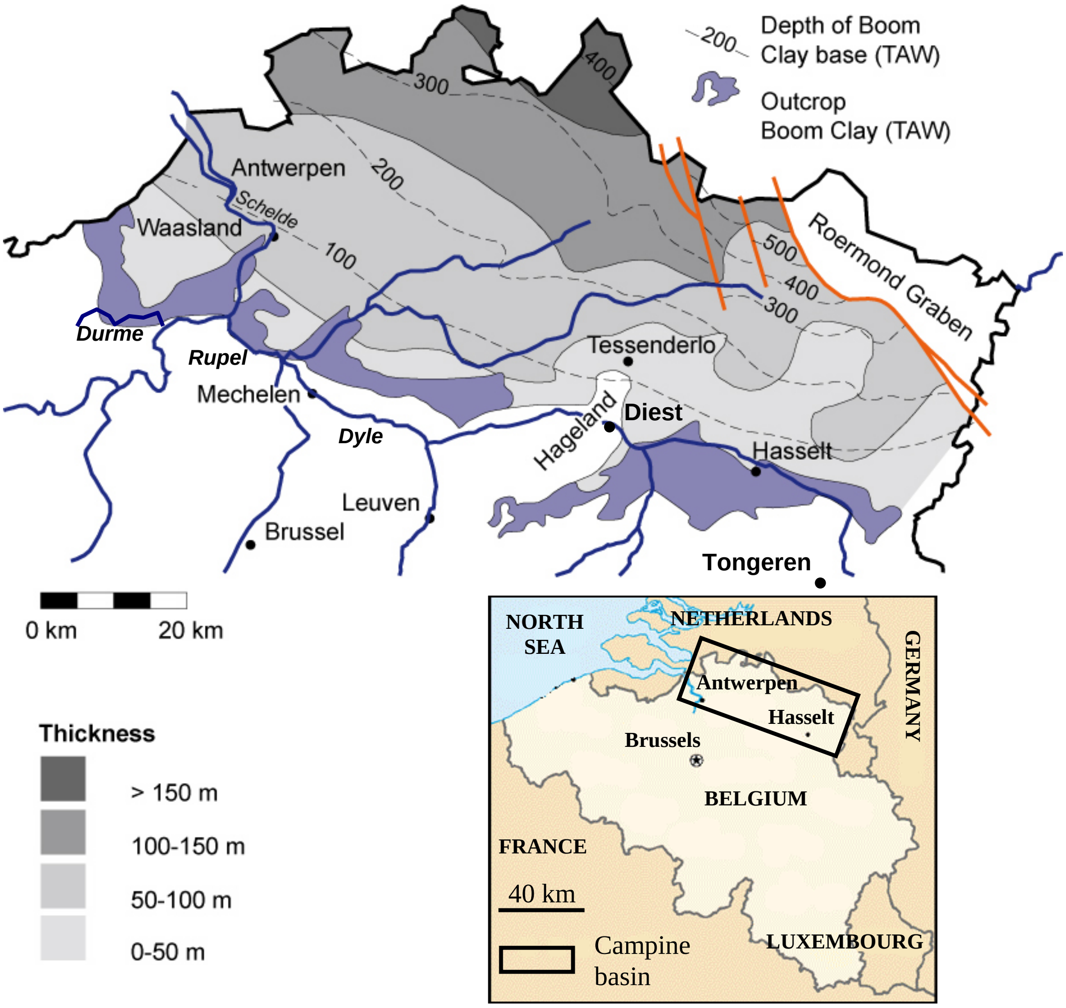

Figure 1.1. Geographical extent, depth and thickness of the Boom Clay in Belgium. TAW: Tweede Algemene Waterpassing, refers to the reference topographic level (zero level) in Belgium (2001, from Safir 2).

In the Rupel region, the type area of the Boom Clay, the formation has been studied in detail in the clay pits where it is intensively exploited for brick-manufacturing. However, the entire stratigraphic sequence of the formation is not present in the outcrop area as the top layers are lacking due to erosion in the course of a continental episode during the Chattian stage. It can be estimated that several tens of meters of the Boom Clay were eroded. The thickness of the Boom Formation in the outcrop area ranges from 30 to 50 m (Wouters and Vandenberghe, 1994).

The Boom Clay gently dips (1-2 %) and thickens towards the northeast. Under the facilities of the SCK•CEN at Mol, the Boom Formation is about 100 m thick and is located at a depth of -190 m to -293 m. The increasing of thickness to the northeast is explained by a less pronounced erosion and a bigger amount of sediments in this direction, which corresponds to that of the basin deepening (Wouters and Vandenberghe, 1994).

1.2 Stratigraphy

The Boom Formation is a Rupelian stage (Lower Oligocene) siliciclastic sediment. The Rupelian stage now comprises the former Rupelian and also part of the continental deposits of the former Tongrian (Table 1.1).

Table 1.1. Chrono- and lithostratigraphy table of the Oligocene (Geets *et al.*, 2003).

Chrono-stratigraphy		**Old name**	**Ma**	**Litho-stratigraphy**
Serie	**Stage**		28.4	**Group**
Oligocene	Chattian		23.8	
	Rupelian	Rupelian		Rupel
		Tongrian		Tongeren
Eocene	Priabonian		33.6	

The Boom Formation forms, together with the Bilzen and Eigenbilzen Formations, the Rupel Group. In the Boom Clay three lithostratigraphic members have been recognised: the lower silt-rich Belsele-Waas Member, the grey clays of the Terhagen Member and the upper dark clays of the Putte Member (Table 1.2). The three Members of the Boom Clay are described in Vandenberghe (1978), Marechal and Laga (1988), Wouters and Vandenberghe (1994) and Vandenberghe (2003).

The Belsele-Waas Member is the lowest and more silty part of the Boom Formation. Its characteristics are the absence of organic-rich black beds, and the occurrence at its bottom of two thick silty layers showing gully type structures. The top of this member is formed by the septaria layer S10. The thickness of the Belsele-Waas Member is usually 10 m. However, it is absent in the most southern part of the outcrop area. The deposition of this member started with a marine transgression 32.7 million years ago (Berggren *et al.*, 1995).

The increasing water depth resulted in the deposition of the Terhagen Member, a gradually finer clay sediment. It constitutes the less silty part of the Boom Formation with only two well-pronounced black beds in the lower part. This member is mainly composed of a “grey clay”. Its top is situated above the septaria level S40 and constitutes the border with the “black clay” of the Putte Member. The thickness of the Terhagen Member is about 20 m in the type area (Rupel region).

The organic-rich upper part of the Boom Clay is the Putte Member. At its bottom, the deposition of coarser sediments known as the “double band” results from a small regression. Later, finer sediments were again deposited due to a second transgressive pulse. The maximum water depth of this transgression corresponds to the septaria level S60. The Putte Member is mainly characterised by the occurrence of black horizons. The clay is darker and more silty than that of the Terhagen Member. The Putte Member is about 40 m thick in the outcrop area. The deposition of the clays finished 28.5 million years ago by the sedimentation of the Eigenbilzen Sands.

Table 1.2. Lithostratigraphy of the Rupel Group (from Vandenberghe, 2003).

Group	Formation	Member	Lithology
Rupel	Eigenbilzen		Fine clayey glauconite-rich bioturbated sands
	Boom	Putte	Dark, blackish-brown organic-rich clays
		Terhagen	Blueish grey to grey, partially carbonate-rich clay
		Belsele-Waas	Grey silty clay
	Bilzen	Kerniel	Fine- to medium-grained whitish-yellowish to brownish quartz sand
		Kleine-Spouwen	Greenish to yellowish grey clay containing carbonate concretions and Nucula compta
		Berg	Yellow to white homogeneous quartz sands

1.3 Lithology

The most striking characteristic of the Boom Clay is its layered structure. This layering is the result of variation in grain size, organic matter and carbonate content as illustrated in Figure 1.2. The observed cyclicity is mostly attributed to glacio-eustatism and tectonism (Van Echelpoel, 1991).

The rhythmicity of the content in clay and silt is the main cause for the banded structure. A clayey bed alternates with a silty bed about every 40 cm. Grain-size analysis of silty and clayey horizons shows that the maximum grain-size in both types of horizons is almost the same. Only the grain-size distribution differs: clayey horizons contain relatively less coarse grains (≥ 16 µm) than silty horizons and conversely. The highest and the lowest percentage of coarse grains are located in the middle of silty and clayey layers, respectively. Moreover, variations in grain-size are gradual (Vandenberghe and Van Echelpoel, 1987). These gradual grain-size variations are related to periodical fluctuations of the bottom turbulence, due to changes in the wave activity. Silt-rich sedimentation is the result of enhanced bottom turbulence while clay-rich sedimentation occurs with decreasing bottom turbulence (Vandenberghe, 1978; Vandenberghe and Van Echelpoel, 1987).

Besides the grain-size variations, black beds are present in the Boom Clay. They all appear grouped together in the upper part of the clay except two beds. Therefore, a feature of the Boom Clay is that it can be subdivided in a lower grey clay, 0.5 to 2 % organic matter and in an upper black clay, 0.5 to 5 % organic matter (Vandenberghe, 1978 and Van Geet *et al.*, 2003). The black beds are sharply limited and occur nearly always immediately above a silty horizon. Their occurrence reflects a higher content in organic matter. Based on the C/N analyses, Vandenberghe (1978) concluded that the black horizons are due to a greater input of terrestrial plant remains, superposed on a constant input of organic matter of marine origin. The appearance of black layers can be explained by the flooding and destruction of coastal vegetation during relative sea-level rise resulting in an increasing flux of continental organic matter. The marine primary production of organic matter might have been higher too during these periods of strong marine influence (Laenen, 1997).

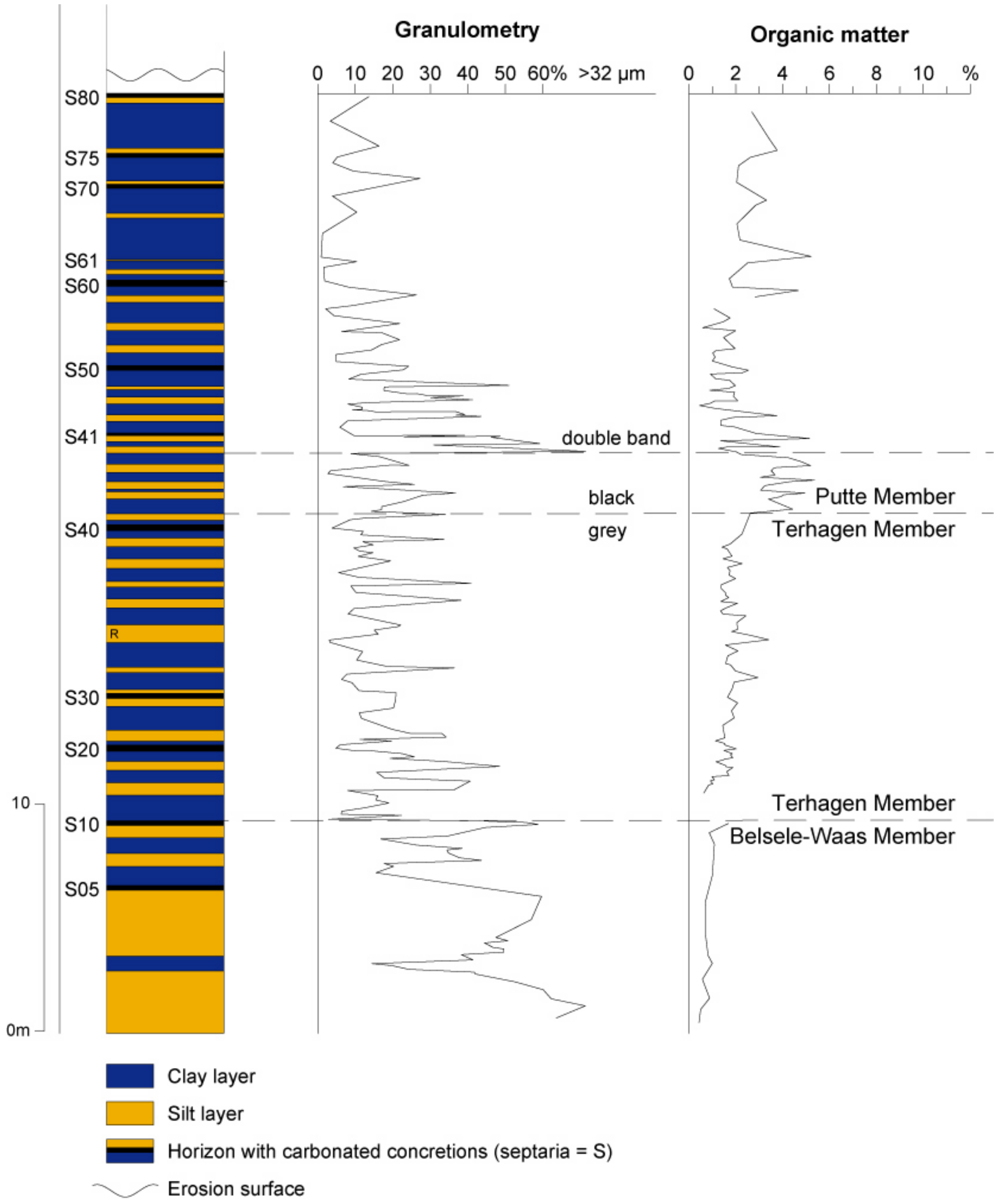

Figure 1.2. Lithostratigraphic profile of the Boom Clay and lithological variations (2001, from Safir 2).

A third rhythmicity results in calcareous-rich horizons in which septarian carbonate concretions often occur. The calcareous layers are characterised by a higher abundance and diversity of calcareous macro- and microfossils compared to the surrounding lithology. This suggests that blooming events of carbonate precipitating organisms occurred (De Craen *et al.*, 1999). The position of these calcareous-rich layers seems not to be related to the organic matter and neither to the grain size since they occur both in clayey and silty horizons (Vandenberghe, 1978; Van Echelpoel, 1991). According to Laenen (1997), their occurrence could be explained by glacio-eustasy: the position of the calcareous layers is generally at the base of major flooding events. Concretions of different levels differ in frequency, dimension, shape, degree of burrow activity and mineralogy. Therefore, their features are used for the lithostratigraphic correlations. In total, 25 concretion-bearing horizons have been identified (Van Keer and De Craen, 2001). They are identified as ”S”-horizons, for example S10, S20, ... (Vandenberghe, 1978).

Other remarkable levels of the Boom Clay are the Double Band (DB) and the pink horizon (R). The Double Band occurs in the lower part of the Putte Member (Figure 1.2). It is formed by two decimetric silty to very fine sandy layers separated by a clayey band. The pink horizon is a more or less 1 m thick silty bed with a pinkish to reddish brown colour occurring in the middle of the Terhagen Member (Figure 1.2). At its base a thin white layer, a few centimeters thick, is present (Vandenberghe, 1978).

1.4 Mineralogy

The detrital mineralogy of Boom Clay mainly consists of clay minerals (30-70 wt. %), quartz (15-60 wt. %) and feldspars (1-10 wt. %). Other detrital minerals which occur in minor amounts are micas and heavy minerals. The clay mineralogy is dominated by illite, smectite, illite-smectite mixed-layer and kaolinite. The authigenic mineral assemblage in the Boom Clay includes glauconite (0-5 wt. %), pyrite (1-5 wt. %), carbonates (1-5 wt. %) and traces of authigenic quartz. Biogenic minerals are apatite, aragonite and quartz occurring as shark teeth, bivalve shells and sponge fragments, respectively. Gypsum (0-1 wt. %) may be present as a weathering product. An overview of the Boom Clay mineralogy is given in the Table 1.3. The organic matter is another important detrital constituent. Indeed, the organic carbon represents up to 5 wt. %. The organic matter will be discussed more in detail later in this chapter.

Table 1.3. Mineralogical composition of the Boom Clay in weight percentage; n: number of samples; min.: minimum; max.: maximum; Mol-1 refers to the Mol-1 borehole.

	Decleer		**Griffault**	**Laenen**		**Wouters**		**De Craen**	
	et.al		***et al.***	**1997**		***et al.***		***et al.***	
	1983		**1996**			**1999**		**2000**	
	n = 21		**n = 11**	**n = 8**		**n = 6**		**n = 36 (Mol-1)**	
	weight %		**weight %**	**weight %**		**weight %**		**weight %**	
	min.	**max.**		**min.**	**max.**	**min.**	**max.**	**min.**	**max.**
Clay minerals	37	71	58	13.6	72.6	30.9*	71.0*	11.4	83.0
Kaolinite	1.0	9.0	10			4.9	13.5	1	15
Illite	3.0	23	17			17.0	43.5	10#	30#
Smectite	19	42				5.5	12.5	10§	30§
Chlorite			2					1	5
Illite/Smectite			29						
Quartz	23.8	58.3	20	16.1	60.3	14.9	52.9	22.0	72.0
Albite	3.2	6.2	2.8	0.1	10.6	2.5	5.2	0.0	11.3
K-feldspar	6.5	11.3	6	0.7	9.9	1.5	4.9	0.0	17.3
Calcite	0.0	4.3	1	0.0	14.6	0.0	3.0	0.0	18.1
Dolomite			0.9			0.0	0.0		
Siderite			0.4	0.0	2.8	0.0	0.3	0.0	2.0
Aragonite						0.0	1.4		
Magnesite						0.0	1.9		
Micas				0.0	2.3	0.0	4.2		
Pyrite	0.7	2.5	4.2	0.66	2.48	0.6	3.5	0.2	8.9
Gypsum						0.0	0.7		
Glauconite				0.01	1.10	2.1	4.8		
Hematite			2.7			0.0	0.1		
Rutile			1.0	0.62	1.06				
Apatite			0.1	0.08	0.58			0.0	1.6

* clay minerals and glauconite

\# illite and muscovite

§ smectite + illite/smectite mixed-layer

1.4.1 Clay mineralogy

It is generally agreed that the clay mineralogy is dominated by illite, illite-smectite mixed-layer and kaolinite. Chlorite, degraded chlorite and illite-chlorite mixed-layer were only found in small amounts (Table 1.4). Less unanimity exists about the contribution of smectite (Laenen, 1997). Decleer *et al.* (1983) reported up to 70 wt. % of smectite while according to Griffault *et al.* (1996) only illite-smectite mixed-layer is present. The presence of vermiculite was debated. On the one hand, Thorez (1976) mentioned the presence of vermiculite and the absence of kaolinite. On the other hand, Vandenberghe (1978) illustrated the presence of kaolinite, while the occurrence of vermiculite was not mentioned. The results obtained by Vandenberghe and Thorez (1985) to identify the possible occurrence of vermiculite did not indicate the presence of this mineral. Griffault *et al.* (1996) mention that the magnesium content in the Boom Clay is too low to form vermiculite.

Van Keer and De Craen (2001) have summarised the available semi-quantitative clay percentages in the literature. The relative percentages of the clay content in the fraction lower than 2 μm are: 6-60 wt. % illite, 0-70 wt. % smectite, 0-50 wt. % of illite-smectite mixed-layer, 10-45 wt. % kaolinite and 1-15 wt. % chlorite. The differences existing from one author to the other in the reported semi-quantitative clay percentages are mainly due to the application of different quantification methodologies. The detailed quantification of the various clay minerals present remains uncertain.

In general, clay authigenesis is considered to be insignificant due to the shallow maximal burial depth of the Boom Clay (Vandenberghe, 1978, Laenen, 1997).

Table 1.4. Clay mineralogical composition of the Boom Clay in weight percentage. Clay mineral amounts are given as relative percentages of the total clay content in the <2 μm fraction; n: number of samples; min: minimum; max: maximum

	Vandenberghe 1978 n = 30 weight %			**Decleer *et al.* 1983 n = 21 weight %**	**Griffault *et al.* 1996 n = 4 weight %**	**Laenen 1997 n = 210 weight %**
	min	**max**	**mean**	**average**	**average**	**average**
Kaolinite	10	31	19	10	19	30
Illite	37	59	48	24	34	19
Smectite	9	28	16	66		40
Illite/Smectite	0	27	12		38	9
Chlorite/Smectite					traces	
Chlorite	2	14	6		9	3

1.4.2 Non-clay mineralogy

1.4.2.1 Quartz

Quartz is the most abundant non-clay mineral. The detrital quartz grains are mainly monocrystalline, equidimensional and angular. Well rounded grains or sharp splinters are less frequent. Some quartz grains contain apatite and rutile inclusions (Vandenberghe, 1978; Zimmerle, 1993).

1.4.2.2 Feldspars

Feldspars mostly occur as angular cleavage fragments without alteration phenomena. Untwinned K-feldspar is more abundant than finely twinned plagioclase. Many feldspars are characterised by minute rutile inclusions or by zonal growth outlined by opaque pigment (Zimmerle, 1993).

1.4.2.3 Micas

Most of the mica consists of muscovite; biotite and altered biotite are less common. The mica flakes are exceptionally large (length up to 300 μm). Biotite is mostly degraded to microcrystalline aggregates of clay minerals, limonite, leucoxene/rutile and carbonate minerals (Zimmerle, 1993).

1.4.2.4 Heavy minerals

The heavy minerals of Boom Clay have been studied by Vandenberghe (1978) and Jedwab and Nicaise (1989). The study by Jedwab and Nicaise confirms most of the minerals recognised by Vandenberghe such as zircon, rutile, anatase, ilmenite, sphene, tourmaline, kyanite, garnet and pyroxenes. However, they have not found andalousite, staurolite, epidote and hornblende. Moreover, they have also determined galena, bravoite, cinnabar, mispickel, xenotime, monazite, chromite, barite, siderite and hydrozincite. Zimmerle (1998) has recognised the following heavy minerals in thin sections: garnet, andalusite, staurolite, kyanite, minerals of the epidote group, spinel, hornblende, zircon, tourmaline and a wide spectrum of TiO_2 minerals (sphene, rutile, anatase, brookite, and leucoxene). An overview of the heavy minerals identified is given in Table 1.5.

Table 1.5. Heavy mineral assemblage of the Boom Clay (Vandenberghe, 1978; Jedwab and Nicaise, 1989; Zimmerle, 1998).

Mineral names	Chemical formula
Galena	PbS
Bravoïte	$(Co,Ni,Fe,Cu)S_2$
Cinnaber	HgS
Mispickel	$FeAsS$
Xenotime	YPO_4
Xenotime - U	$(Y,U)PO_4$
Monazite - Ce	$(Ce,La,Nd,Th)PO_4$
Monazite - La	$(La,Ce,Nd)PO_4$
Hydrozincite	$Zn_5(CO_3)_2(OH)_6$
Andalusite	Al_2SiO_5
Kyanite	Al_2SiO_5
Spinel	$MgAl_2O_4$
Chromite	$FeCr_2O_4$
Rutile-anatase	TiO_2
Brookite	TiO_2
Sphene	$CaTiSiO_5$
Ilmenite	$FeTiO_3$
Leucoxene	alteration product of Ti-bearing minerals
Zircon	$ZrSiO_4$
Barite	$BaSO_4$
Baryto-celestite	$(Ba,Sr)SO_4$
Staurolite	$FeAl_9O_6(SiO_4)_4(O,OH)_2$
Epidote	$Ca_2(Al,Fe)Al_2O(SiO_4)(Si_2O_7)(OH)$
Hornblende	$(Ca,Na)_{2-3}(Mg,Fe,Al)_5Si_6(Si,Al)_2O_{22}(OH)_2$
Pyroxene	$XY(Si,Al)_2O_6$ with X:Na,Ca,Mn,Fe,Mg,Li; Y: Mn,Fe,Al,Cr, Ti
Tourmaline	$(Na,Ca)(Li,Mg,Al)_3(Al,Fe,Mn)_6(BO_3)_3(Si_6O_{18})(OH)_4$

1.4.3 Authigenic minerals

1.4.3.1 Glauconite

Glauconite is mainly found in the most silty layers of the Boom Clay. It is generally absent from the Terhagen Member. The authigenic character is proved by the modal size of the glauconite which is larger than that of detrital grains. Two kinds of glauconite are present (Vandenberghe, 1978):

- light greenish glauconite is the predominant type. The grains, ranging between 75 and 150 μm, are mostly spherical and rounded, without lobes. Sometimes surface cracks are observed, resulting in a rather rough surface. Quartz grains and muscovite flakes are often found as inclusions,
- dark green glauconite grains have a minimal size between 125 and 150 μm. They are lobed and always show a smooth surface. The ridges between the lobes can be filled with light green glauconite. Small dark green glauconite can also be included in a large light green glauconite.

Glauconite coatings are found on pyrite fragments, kyanite and quartz grains. According to Laenen (1997), glauconitisation starts with the nucleation of Fe-oxyhydroxides in pores of the substratum. Subsequently, these Fe-oxyhydroxides directly transform into glauconitic smectite. Further evolution towards illitic glauconite is controlled by the reduction of ferric iron and cation exchange. The glauconite found in the Boom Clay presents a mineralogy ranging from a smectitic to an illitic composition.

1.4.3.2 Pyrite

In the Boom Clay, different types of pyrite have been determined and described by Vandenberghe (1978) and De Craen (1998). Pyrite is predominantly present as framboids, although discrete octahedral pyrite crystals also frequently occur (Figure 1.3). Both are dispersed in the clay matrix. Four types of framboids have been recognised: “normal” framboids (5-20 μm) dominate but “microframboids” (1-3 μm), “megaframboids” (100-250 μm) and “polyframboids” composed of aggregates of smaller framboids are also present. Two types of euhedral pyrite crystals also frequently occur: microcrystalline octahedral pyrite crystals (0.5-1 μm) always associated with the normal framboids, and octahedral pyrite crystals (1-8 μm) which are not related to pyrite framboids.

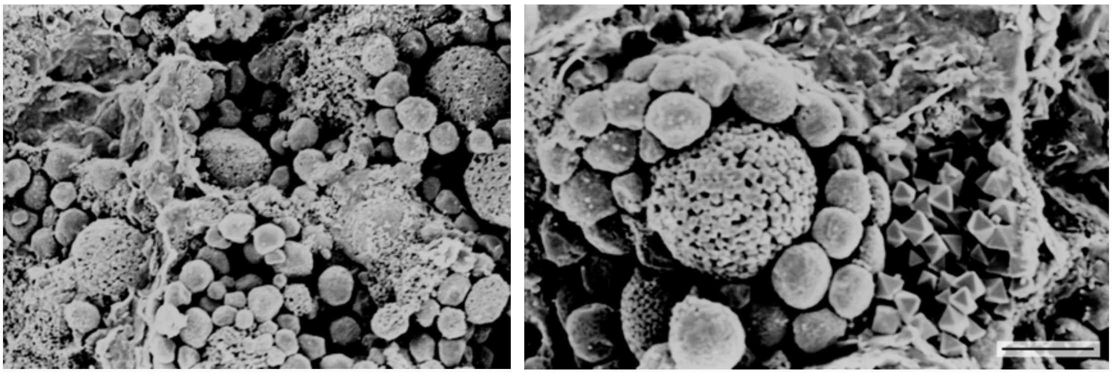

Figure 1.3. Framboidal pyrite and discrete octahedral pyrite crystals in the Boom Clay, scale bar = 10 μm (from De Craen, 1998).

Pyrite is also present as concretionary bodies (Figure 1.4): cylindrical pyritised worm tubes (few cm), large elongated concretionary worm tubes (up to 10 cm) with a nodular aspect, spherical pyrite nodules, small pyrite aggregates (< 2 cm), and layered pyrite. Concretionary pyrite bodies are mostly composed of amorphous pyrite and octahedral pyrite crystals. The occurrences of pyrite suggest a close relationship with organic forms.

The occurrence of both framboidal pyrite and euhedral crystals reflects two distinct pathways of pyrite formation that are described in De Craen (1998) and references therein. Pyrite formed by bacterially-mediated production of sulphides exhibits a framboidal morphology. Framboidal pyrite is the result of early diagenetic reactions involving bacterial sulphate reduction associated with rapid iron reduction. During sulphate reduction processes, bacteria use the oxygen of sea-water sulphate to metabolise organic matter, resulting in the formation of HCO_3^- and HS^-:

$$2\ CH_2O + SO_4^{2-} \rightleftharpoons H^+ + 2\ HCO_3^- + HS^-$$

The dissolved sulphide reacts with iron bearing detrital minerals to form metastable monosulphide (greigite and mackinawite) together with elementary sulphur:

$$3\ H_2S + Fe_2O_3 \rightleftharpoons 2\ FeS + S + 3\ H_2O$$

Subsequently, rapid reaction of monosulphide with elementary sulphur results in pyrite formation:

$$FeS + S \rightleftharpoons FeS_2$$

Not only anaerobic bacterial sulphate reduction can cause pyrite formation. Pyrite can also be formed by anaerobic methane oxidation which also produces HCO_3^- and HS^-:

$$CH_4 + SO_4^{2-} \rightleftharpoons HCO_3^- + HS^- + H_2O$$

Pyrite formed during anaerobic methane oxidation is characterised by an euhedral non-framboidal morphology. This kind of pyrite most likely formed during a later stage in diagenesis.

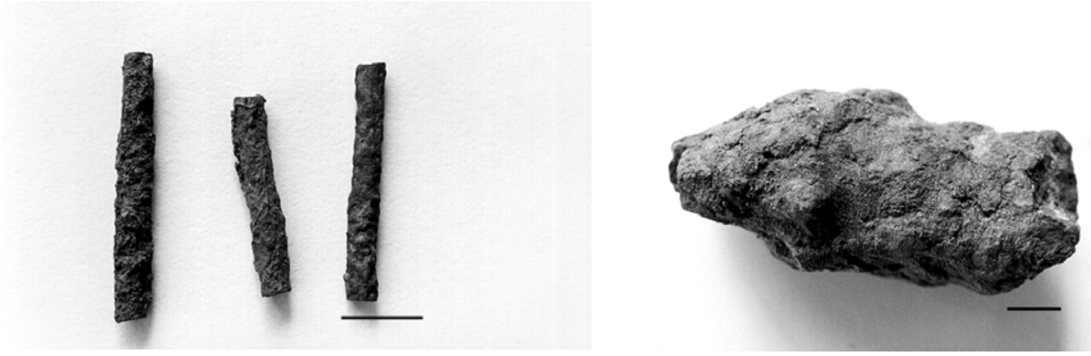

Pyritised worm tubes.
Scale bar = 5 mm

Concretionary worm tube.
Scale bar = 1 cm

Pyrite nodule. Scale bar = 1 cm

Pyrite aggregate. Scale bar = 1 cm

Figure 1.4. Different types of concretionary pyrite bodies recognised in the Boom Clay (from De Craen, 1998)

1.4.3.3 Carbonates

Carbonate authigenesis is most developed in the calcareous layers. Authigenic calcite in the clay mostly occurs as irregular shaped crystals ranging from 1 to 5 μm. Authigenic siderite is present, especially between S50 and S80, as isolated rhombohedral crystals smaller than 10 μm.

In the Boom Clay, the precipitation of carbonate resulted in the formation of carbonate septarian concretions, usually called "septaria". These concretions have been extensively studied by De Craen (1998). They are generally composed of ferroan calcite although the ferroan calcite is accompanied by siderite in the Putte Member (especially in S60 and S80).

The septaria have a flattened spheroidal shape with a diameter between 30 cm and 1 m (or even more), and a thickness between 10 and 20 cm. They are characterised by the presence of a network of fractures, called "septae" from which comes the name septaria (Figure 1.5). In all concretions, septarian fractures are filled with various generations of calcite and/or pyrite cement.

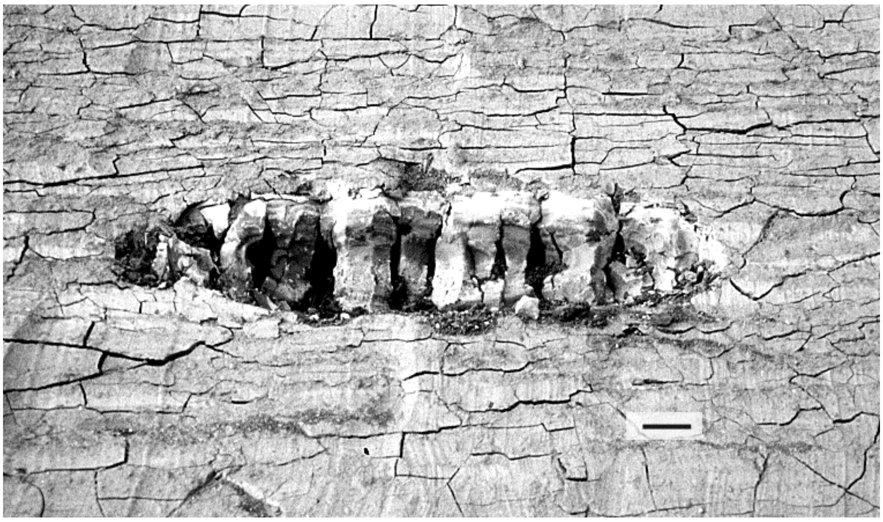

Figure 1.5. Septarian carbonate concretion present in Boom Clay (S40-level), Boom Clay Quarry at Rumst, Belgium. Scale bar = 10 cm (from De Craen, 1998).

The carbonate concretions are composed of a fine-grained matrix containing detrital minerals and fossils, cemented by authigenic carbonates. All the detrital minerals are related to the host sediment. Ostracods, gastropods, foraminifera, coccoliths and molluscs are also part of the concretion matrix. Delicate shell outlines are often well-preserved and do not show any significant compactional deformation, indicating that the concretions were formed early in diagenesis. Framboidal pyrite occurs disseminated throughout the concretion matrix or as infillings in fossils pipes and between faecal pellets. The concretionary carbonate cement, mainly ferroan calcite, is characterised by a micritic to a microsparitic texture with a sub-rhombohedral crystal morphology (1-5 μm). Siderite is also present in the S60 and S80 levels.

The preservation of very delicate features, the isotopic studies and the presence of mineralised bacteria indicate an early lithification, before compaction; with the dominant formation process being bacterially-mediated degradation of organic matter under anaerobic conditions in an open diagenetic system, mainly occurring in the sulphate reduction zone.

1.4.3.4 Quartz

Scanning electron microscopy investigations of the clay in calcareous-rich layers in the lower part of the Putte Member have indicated the presence of authigenic quartz crystals smaller than 5 μm (De Craen, 1998). Auhtigenic quartz has only occasionally been observed.

1.4.4 Biogenic minerals

1.4.4.1 Apatite

Jedwab and Nicaise (1989) have observed phosphate fragments during their study of the minor constituents of the Boom Clay. These fragments are made of calcium phosphate, *i.e.* apatite or collophane. They mainly originate from animals: pieces of teeth, scales, small vertebra, ... have been recognised. Fossil biogenic apatite is mainly present as shark teeth.

1.4.4.2 Aragonite

The bivalve shells occurring in the Boom Clay mostly belong to the species Nucula *deshayesiana* and Nucula *duchasteli*. Species of the genera Astarte, Ostrea and Corbula are also identified. A notable characteristic of the bivalve shells is its aragonitic composition. Aragonite is unstable during meteoric alteration and is more soluble than calcite under low pressure and temperature conditions. Therefore, the bivalve shells composition indicates that they have not been involved in either early diagenesis or weathering processes (Laenen, 1997).

1.4.4.3 Quartz

Zimmerle (1993) has observed fragments of beige or violet greyish, biogenic chalcedony which are considered as siliceous sponge fragments. Interesting to note is the presence of "white spots" of 1-2 mm wide and about 5 mm long in the Putte Member. X-ray diffraction (XRD) has indicated that they are composed of quartz. These "white spots" sometimes form fine lines up to 15 cm long or more. They are interpreted as fossil traces of burrow pipe (Van Simaeys, personal communication).

1.5 Granulometry

The very fine grained nature of the Boom Clay is an important characteristic. In general, detrital grains have sizes below 100 μm. As illustrated in Table 1.6, the samples of the Boom Clay range from sand-silt-clay over clayey silts towards silty clays (Vandenberghe, 1978; Laenen, 1997). The grain size population consists of clayey silts and silty clays. The rhythmic variation of silty beds and clay-rich beds observed in the field is mostly due to a silt and in some cases to a fine sand (> 63 µm) addition to the clayey silts and silty clays. Fine sand addition occurs especially near the base of the Boom Formation (Vandenberghe, 1978). Silt and clay beds only differ in the position of the frequency distribution maximum of the silt population. In the coarsest samples the maximum is in the coarse silt to fine sand range while the clay beds show a maximum towards the fine silt sizes (Laenen, 1997). The very fine size of detrital grains suggests a suspension transport even for the sand fraction (Vandenberghe, 1978).

Table 1.6. Grain-size distribution of Boom Clay samples; n: number of samples, min: minimum; max: maximum; Mol-1 refers to the Mol-1 borehole

Particles diameter (d)	**Granulometric class**	**Decleer *et al.* 1983 n = 21 weight %**		**Laenen 1997 n = 8 weight %**		**De Craen *et al.* 2000 n = 36 (Mol-1) weight %**	
		min	**max**	**min**	**max**	**min**	**max**
$d < 2\ \mu m$	clay	23.5	63.3	26.8	64.5	10.1	58.0
$d < 10\ \mu m$		29.6	82.5				
$d < 20\ \mu m$		32.7	89.0				
$2\ \mu m < d < 63 \mu m$	silt			21.6	45.5	31.8	76.4
$d > 63\ \mu m$	sand	0.5	33.6	3.2	30.6	1.1	25.6
$d > 106\ \mu m$		0.1	4.1				

1.6 Geochemistry

1.6.1 Solid phase

The chemical composition of a clay sediment is a function of its clay mineralogical composition, the quantity of free silica and the presence of varying amounts of minerals such as pyrite and carbonates. In general, variations in major element concentration in the Boom Clay are small suggesting that the geochemical composition of the Boom Clay is more or less constant (Table 1.7). The geochemistry results from mineralogical variations and mostly from mixing of clay and coarse-grained minerals (Vandenberghe, 1978; Decleer, 1983; Laenen, 1997; De Craen *et al.*, 2000).

Laenen (1997) carried out a detailed geochemical characterisation of the Boom Clay bulk sediment, clayey fraction (< 2 μm), glauconite and biogenic apatite (shark teeth).

Two main groups of elements were recognised in the bulk sediment:

- a "silt-group" which contains Na_2O, SiO_2, Hf, Ba and Zr,
- a "clay group" which contains Al_2O_3, Fe_2O_3, FeO, K_2O, MgO, TiO_2, Co, Cr, Nb, Rb, Sc, Ta, Th, Y, Zn and the rare earth elements (REE).

The elements of the "silt-group" are enriched in the coarse fractions (>16 μm) and depleted in the clayey fraction. The correlation with mineralogy suggests that these elements are chiefly incorporated in heavy and coarse minerals, *e.g.* quartz, feldspars, muscovite, glauconite and zircon. The elements of the "clay-group" are enriched in the clay-sized sediment fraction and are associated with the clay minerals. The variations in REE concentration with depth are in general small. The tendency of TiO_2 to be concentrated in the fine particle fraction, probably as anatase, was also noticed by Vandenberghe (1978) and Decleer (1983). Ca, Sr and total inorganic carbon (TIC) correlate with the amount of calcite while total organic carbon (TOC), N and S correlate with the organic matter content. P_2O_5 and MnO do not correlate neither with the grain-size distribution nor with the mineralogy (Laenen, 1997).

The trace element concentrations of the clayey fraction are rather homogeneous. This low variability reflects the minor changes in mineralogy and environmental conditions.

Glauconite is moderately enriched in Co, Cr, Fe, Hf, Sc, Sr, Ta, Th, U and REE compared to the surrounding sediment and clay fraction (Laenen, 1997).

The absolute concentration of the elements measured in the shark teeth appears to depend mainly on properties of the individual tooth samples (porosity, recrystallisation rate) and on the local supply of trace elements from the sediment-seawater interface and from the pore water (Laenen *et al.*, 1997).

The geochemistry of the bulk sediment was also studied by De Craen *et al.* (2000). These authors have identified three main groups to explain the trace elements distribution. Two groups are equivalent to those recognised by Laenen (1997): a group related to the resistant minerals (quartz, feldspars, heavy minerals) which concentrates Zr and a clay group which concentrates Th, light and middle REE, Rb and Cs. The third group contains organic matter, pyrite, calcite and apatite and concentrates heavy REE (Lu) and U.

Table 1.7. Chemical analyses of Boom Clay bulk samples. The concentrations are expressed as weight percentages; min: minimum; max: maximum.

	Vandenberghe 1978 n = 15 weight %		**Decleer *et al.* 1983 n = 21 weight %**		**Griffault *et al.* 1996 n = 11 weight %**		**Laenen 1997 n = 8 weight %**		**De Craen *et al.* 2000 n = 36* weight %**	
	min	**max**	**min**	**max**	**min**	**max**	**min**	**max**	**min**	**max**
SiO_2	39.3	72.86	54.19	73.38	55.70	56.60	55.53	78.21	46.4	73.1
Al_2O_3	0.57	15.94	8.65	18.41	18.60	19.20	7.77	19.58	11.7	20.7
TiO_2	0.57	0.91	0.59	0.99	0.95	0.98	0.58	0.99	0.58	0.86
Fe_2O_3	3.21	6.68	2.18	4.42	2.60	3.65	2.25	4.13	3.11	6.74
FeO	—	—	0.89	1.76	2.20	2.80	0.73	1.72	—	—
MgO	0.98	2.11	0.94	1.34	2.20	2.30	0.81	1.95	1.8	2.6
CaO	0.35	14.56	0.66	3.50	0.67	1.24	0.39	8.05	0.36	7.88
Na_2O	0.21	0.6	0.33	0.50	0.60	0.80	0.22	0.55	0.45	0.70
K_2O	2.49	3.12	2.55	3.31	3.38	3.45	2.08	3.24	2.62	3.53
MnO	0	0.03	—	—	0.02	0.03	0.014	0.025	0.010	0.018
P_2O_5	0.04	0.15	0.08	0.11	0.09	0.12	0.05	0.25	0.07	0.17
SO_3	1.23	4.45	1.15	4.94	—	—	0.87	4.64	0.8	6.2
L.O.I.[#]	6.24	21.36	3.77	11.38	10.17	10.84	—	—	3.03	15.9
Org. C[§]	—	—	0.64	4.50	—	—	0.27	0.59	—	—

* Samples from the Mol-1 borehole
# Loss Of Ignition at 1000°C
§ Organic carbon

1.6.2 Liquid phase

The water content in the Boom Clay determined on 22 saturated cores from the Mol-1 borehole varies from 21.0 to 26.8 wt. % by dry weight, with an average value of 24.4 wt. %. By wet weight, the water content varies between 17.4 and 21.1 wt. % with an average value of 19.6 wt. % (Wemaere *et al.*, 2002).

1.6.2.1 Water composition

The geochemistry of the Boom Clay pore water a the Mol site is discussed in detail by De Craen *et al.* (in preparation). The water composition reported in Table 1.8 is that of the Extension Gallery/Bottom Shaft (EG/BS) water (Dierckx, 1997). This water was used as reference Boom Clay pore water in the laboratory experiments conducted in the framework of this research. The EG/BS piezometer is installed in the underground research laboratory since September of 1983, at a depth of about - 250 m below the surface of the SCK•CEN facilities. It provides large quantities of Boom Clay pore water (about 1 litre a day) and EG/BS water is used already a long time for many laboratory experiments. The Boom Clay water is of the sodium bicarbonate type; $NaHCO_3 \sim 1.5\times10^{-2}$ mol·l^{-1}. Since the water composition given in Table 1.8 is determined under conditions required for the analyses techniques, the reported aqueous species are not necessary those prevailing under the *in situ* Boom Clay conditions. Therefore, Wang *et al.* (2000) computed the water composition adapted for *in situ* conditions (Table 1.8). The phosphate concentration should be lower than that indicated by Dierckx (1997). More recent measurements have shown that the HPO_4^- content is below the detection limit, *i.e.* 2.5 ppm (Wang *et al.*, 2000).

Table 1.8. Average composition of EG/BS water (Dierckx, 1997) and the adapted composition for the *in situ* Boom Clay conditions (Wang *et al.*, 2000).

Reported EG/BS water composition			**Adapted EG/BS water composition**		
	$mg \cdot l^{-1}$	**$mol \cdot l^{-1}$**		**$mg \cdot l^{-1}$**	**$mol \cdot l^{-1}$**
F^-	3.6	1.9×10^{-4}	F^-	3.6	1.9×10^{-4}
Cl^-	27	7.6×10^{-4}	Cl^-	27	7.6×10^{-4}
SO_4^{2-}	0.2	2.1×10^{-6}	SO_4^{2-}	0.2	2.1×10^{-6}
Br^-	0.49	6.1×10^{-6}	Br^-	0.49	6.1×10^{-6}
HPO_4^{2-}	3.8	4.0×10^{-5}	HPO_4^{2-}	<2.5	$<2.6 \times 10^{-5}$
HCO_3^-	828	1.4×10^{-2}	—	—	—
B	7.5	6.9×10^{-4}	$B(OH)_3(aq)$	42.90	6.9×10^{-4}
Na	408	1.8×10^{-2}	Na^+	408	1.8×10^{-2}
Mg	2.9	1.2×10^{-4}	Mg^{2+}	2.9	1.2×10^{-4}
Al	0.08	2.9×10^{-6}	AlO_2^-	0.17	2.9×10^{-6}
Si	5	1.8×10^{-4}	$SiO_2(aq)$	10.7	$1.8\ 10^{-4}$
K	11	2.8×10^{-4}	K^+	11	2.8×10^{-4}
Ca	4.0	9.9×10^{-5}	Ca^{2+}	4.0	9.9×10^{-5}
Fe	0.9	1.6×10^{-5}	$FeHCO_3^+/FeCO_3(aq)$	1.88	1.6×10^{-5}
			pCO_2, atm	$10^{-2.42}$ (16°C)	
			E_h, mV	- 275	
			*p*H	8.2	

1.6.2.2 Partial pressure of CO_2

The only measurement of partial pressure of CO_2 (pCO_2) on Boom Clay was performed by Henrion *et al.* (1985) who reported a value of $10^{-2.5}$ atm. The measurement was not carried out under *in situ* conditions but on frozen clay samples in surface laboratory at 25°C. Dierckx (in Aertsens *et al.*, 1995) calculated a pCO_2 of $10^{-2.42}$ atm at *p*H 8.2 and 16°C assuming that the total inorganic carbon content was controlled by the solubility of CO_2 in the clay water. This value agrees relatively well with that measured by Henrion *et al.* (1985). The partial pressure of CO_2 can also be calculated on the basis of likely processes controlling this parameter. Values of pCO_2 of $10^{-3.1}$ to about $10^{-2.5}$ atm were estimated by assuming that pCO_2 is constrained either by calcite equilibrium with water or by mineral assemblages (De Craen *et al.*, in preparation).

At the time of this research, pCO_2 of $10^{-2.42}$ atm is considered as the reference value for the Boom Clay. The pCO_2 of the Boom Clay is about 10 times higher than the atmospheric pCO_2 ($10^{-3.5}$ atm). Therefore, any contact with air tends to lower the pCO_2 due to the loss of dissolved CO_2 by re-equilibrium with the atmospheric pCO_2.

1.6.2.3 pH

Because of the oversaturation of CO_2 in Boom Clay pore water with respect to atmospheric conditions, special precaution must be taken during *p*H measurement to avoid degassing of the pore water. The loss of CO_2 will increase *p*H. Griffault *et al.* (1996) measured a *p*H value of 8.20 ± 0.05 under *in situ* conditions at a pressure of 17.6 bar (see also Beaucaire *et al.*, 2000). This value was obtained using an optical sensor and a coloured *p*H indicator adsorbed on a bead of resin tightened at the end of an optical fibre. Recent *in situ* measurements at about 18 bar of water pressure revealed a *p*H value of 8.0 ± 0.2 (Moors *et al.*, 2002). The measurement was performed with a pressure resisting *p*H electrode filled with solid polymer (Xerolyt, Mettler-Toledo). An alternative way to acquire *p*H of Boom Clay is through speciation calculation. Assuming a chemical equilibrium between calcite and the pore water, *p*H values between 8.3 and about 8.6 are estimated (De Craen *et al.*, in preparation).

So far, *p*H of 8.2 is generally accepted as the reference value for Boom Clay pore water. Higher *p*H values are due to a degassing of the dissolved CO_2. Boom Clay pore water should have a *p*H of about 9.3 by assuming equilibration with air (Beaucaire e*t al.*, 2000; De Craen *et al.*, in preparation). The initial step of degassing is quite fast: within an hour, the *p*H increases about a half *p*H unit. The equilibrium value of 9.3 is approached after 48 hours of contact with air under a strong mechanical stirring (De Craen *et al.*, in preparation).

1.6.2.4 Redox potential

Due to the presence of organic matter and minerals such as pyrite and siderite, the Boom Clay is a reducing environment and has negative redox potential (E_h). According to Berner's classification (1981), the Boom Clay is an example of an anoxic nonsulphidic environment. The concentration of total dissolved sulphide in Boom Clay pore water is lower than 10^{-6} $mol{\cdot}l^{-1}$ (Beaucaire *et al.*, 2000). This concentration is too low to classify the Boom Clay as a sulphidic environment. Boom Clay phases such as pyrite, siderite and organic matter are characteristic of a methanic environment which suggests highly reducing conditions.

The redox potential of the Boom Clay has been reported in the range -250 to -400 mV according to *in situ* measurements (Henrion *et al.*, 1985; Beaufays *et al.*, 1994; Aertsens *et al.*, 1995). Recent E_h measurement at the *in situ* hydraulic pressure give a redox potential of -310 ± 30 mV (Moors et *al.*, 2002). This wide range of reported values is due to the fact that redox potential measurements in such poorly buffered fluids as deep pore waters are always very delicate and can be misleading (Stumm and Morgan, 1996). The very low concentration of electroactive species (Fe^{2+}, HS^-, ...) in the pore water collected from the piezometer explains the difficulty to unquestionably measure the redox potential.

Although redox potential of the Boom Clay has been proven difficult to measure and interpret, plausible processes controlling the E_h can be anticipated from using the E_h-*p*H diagram. Based on a combined *p*E-*p*H diagram for iron and sulphur, Beaucaire *et al.* (2000) calculated that the clay water potential is lower than -220 mV *vs* SHE.

The current-state conceptual model for describing redox processes in the Boom Clay suggests that the measured E_h is probably controlled by the equilibrium of pyrite and siderite (De Craen *et al.*, in preparation):

$$FeS_2 + 9H_2O + CO_2 \rightleftharpoons 18H^+ + 2SO_4^{2-} + FeCO_3 + 14e^-$$

Under Boom Clay condition (pCO_2 of $10^{-2.4}$ atm, and sulphate concentration of about 10^{-6} mol·l^{-1}), the following E_h-*p*H relationship can be derived:

$$E_h\ (V) = -\ 0.076\ pH + 0.34$$

At *p*H = 8.2, the redox potential is -283 mV which is the upper limit of the pyrite stability field. Lower redox potentials are possible as the result of interactions involving organic matter mediated by biochemical processes.

1.7 Organic matter

Organic matter is an important constituent of the Boom Clay. Two types of organic matter are distinguished: the insoluble (kerogen) and the soluble. The kerogen fraction represents up to 5 wt. % of the Boom Clay. This solid phase organic matter is immobile since present within the clay matrix. The soluble fraction is dissolved in Boom Clay pore water and, therefore, considered as mobile. The concentration of total organic carbon (TOC) in Boom Clay pore water is about 100 mg·l^{-1}. Assuming that the Boom Clay contains 20 % of water, 2 % of kerogen and 100 mg·l^{-1} of dissolved organic carbon, about 99.9 % of the organic matter occur as insoluble kerogen while about only 0.1 % is dissolved.

An overview of all available literature data on the organic matter present in the Boom Clay is given by Van Geet *et al.* (2003) and references therein.

1.7.1 Insoluble organic matter

Deniau *et al.* (2001) studied the immobile Boom Clay organic matter by scanning and transmission electron microscopy. These studies showed that Boom Clay organic matter is mainly amorphous, composed of aggregates of various sizes (from 30 to 200 μm) without well-defined shapes. There was no close association with the mineral matrix observed, neither regular organo-mineral organisation, nor a thin coating of mineral grains.

Vandenberghe (1978) reported a C/N ratio varying between 5 and 23.8 through the Boom Clay. He concluded that the C/N ratios of the bulk sediment are the result of mixing a pool of N-poor organic matter of terrestrial origin and a N-rich organic matter pool with a marine origin. Moreover, the C/N ratio increases together with the organic carbon content. This positive correlation may indicate that the increase in organic matter was due to an increase of the terrestrial input. This interpretation was confirmed by Van Geet (2002) who discriminates two populations of insoluble organic matter. The first population has TOC values below 2 % and is omnipresent throughout the Boom Clay. The second population has TOC values above 2 % and is limited to the Putte Member, especially the zone between the Terhagen-Putte boundary and the septaria level S50. The first population derived mainly from terrestrial organic matter (higher plants and reworked coal fragments) but also from algae. The second population has the highest proportional contribution of autochthonous marine organic matter but at the same time the highest absolute concentration of both marine and terrestrial pools of organic matter (Van Geet *et al.*, 2003).

The organic matter present in the Boom Clay is immature since all maturity parameters show a low maturity and do not present any variation through the section (Laenen, 1997).

1.7.2 Soluble organic matter

Little is known about the mobile organic matter present within Boom Clay pore water (Van Geet *et al.*, 2003). The soluble organic matter in piezometer water gives TOC values between 95 and 265 $mg \cdot l^{-1}$ (De Craen *et al.* in preparation). A mean TOC content of 115 ± 15 $mg \cdot l^{-1}$ seems the most representative value. According to Maes *et al.* (2003), the soluble organic matter comes from an easily soluble organic matter pool, but also from an organic matter fraction for which the release is dictated by an adsorption mechanism.

Three fractions of aquatic humic substances are defined, based on their solubilities in acids and base. These include fulvic acids, which are soluble in both acid and alkaline solutions, humic acids are soluble in alkaline solutions, but insoluble in acid and humin is insoluble in acid or alkaline solutions (Stevenson, 1982). Concentrates of organic matter from Boom Clay pore water contain about 70 % of humic acids and 30 % of fulvic acids (Dierckx *et al.*, 2000). The aquatic humic substances are operationally defined as polyelectrolytic acids composed of about 50 % C, 35 to 40 % O, 4 to 5% H, and 1% N (Langmuir, 1997). In general, fulvic acids fall in the 500-2000 dalton range and humic acids in the 1000-10000 dalton range (Choppin, 1992) although the determination of molecular size is a complex matter. In the Boom Clay, the size distribution of soluble organic matter is varying about 1000 dalton but sizes above 100000 dalton have been measured as well (Van Geet *et al.*, 2003).

1.8 References

Aertsens, M., De Cannière, P., Dierckx, A., Fonteyne, A., Moors, H., Ortiz, L., Put, M., Van Gompel, M., Wang, L. 1995. Geological disposal of conditioned high-level and long lived radioactive waste – Tasks 1.2 to 5.2 & Operation and maintenance of the URF. Progress report to NIRAS/ONDRAF for the first semester of 1995, Task 2.1, 2.3, and 2.4: Migration studies. SCK•CEN report, **R 3080 Volume 2 (of 3)**, Mol, Belgium.

Beaucaire, C., Pitsch, H., Toulhoat, P., Motellier, S., Louvat, D. 2002. Regional fluid characterisation and modelling of water-rock equilibria in the Boom Clay formation and in the Rupelian aquifer at Mol, Belgium. *Applied geochemistry* **15**, 667-686.

Beaufays, R., De Cannière, P., Fonteyne, A., Labat, S., Meynendonckx, P., Noynaert, L., Volckaert, G., Bruggeman, A., Lambrechts, M., Vandervoort, F. 1994. Cerberus: a demonstration test to study the near field effects of an HLW canister in argillaceous formation. European Commission Nuclear Science and Technology. Final report **EUR 15718** EN.

Berggren, W.A., Kent, D.V., Swisher, C.C., Aubry, M.P. 1995. A revised Cenozoic Geochronology and Chronostratigraphy. *In*: " Geochronology, Time scales and global stratigraphic correlation" (Berggren, W.A., Ken,t D.V., Aubry, M.P.,Hardenbol J. eds.). Society of Economic Paleontologists and Mineralogists, Special Publication, **54**, 129-212.

Berner, R.A. 1981. A new geochemical classification of sedimentary environments. *Journal of Sedimentary Petrology*, **51/2**, 359-365.

Choppin, G.R. 1992. The role of natural organic in radionuclide migration in natural aquifer systems. *Radiochimica Acta* **58/59**, 113-120.

De Craen, M. 1998. "The formation of septarian carbonate concretions in organic-rich argillaceous sediments". Ph.D. thesis, K.U.Leuven, Leuven, Belgium.

De Craen, M. Swennen, R., Keppens, E.M., Macaulay, C.I., Kiriakoulakis, K. 1999. Bacterially mediated formation of carbonate concretions in the Oligocene Boom Clay of northern Belgium. *Journal of sedimentary research* **69/5**, 1098-1106.

De Craen, M., Delleuze, D., Volckaert, G., Sneyers, A., Put, M. 2000. The Boom Clay as natural analogue. SCK•CEN report, **R-3444**, Mol, Belgium.

De Craen, M., Wang, L., Van Geet, M., Moors, H. 2004. Geochemistry of the Boom Clay pore water a the Mol site. SCK•CEN report, **BLG-xxx**, Mol, Belgium. *In preparation.*

Decleer, J., Viaene, W., Vandenberghe, N. 1983. Relationships between chemical, physical and mineralogical characteristics of the rupelian Boom Clay, Belgium. *Clay Minerals* **18**, 1-10.

Deniau, I., Derenne, S., Beaucaire, C., Pitsch, H., Largeau, C. 2001. Morphological and chemical features of a kerogen from the underground Mol laboratory (Boom Formation, Oligocene, Belgium): structure, source organisms and formation pathways. *Organic Geochemistry* **32**, 1343-1356.

Dierckx, A. 1997. Boom Clay in situ pore water chemistry. SCK•CEN report, **BLG-734**, Mol, Belgium.

Dierckx, A., Put, M., De Cannière P., Wang, L., Maes, N., Aertsens, M., Maes, A., Vancluysen, J., Verdickt, W., Gielen, R., Christiaens, M., Warwick, P., Hall, A., Van der Lee, J. 2000. Transport of radionuclides due to complexation woth organic matter in clay formations (Trancom-Clay). European Commission Nuclear Science and Technology. Final report **EUR 19135** EN.

Geets S., Maréchal, M., Laga P., De Ceuckelaire M., Gouwy, S. 2003. Table of the lithostratigraphy of the Paleogene in Belgium. In "Symposium on the Paleogene, preparing for modern life and climate". August 25-30, 2003, Leuven, Belgium.

Griffault, L., Merceron, T., Mossmann, J.R., Neerdael, B., De Cannière, P., Beaucaire, C., Daumas, S., Bianchi, A., Christen, R. 1996. Acquisition et régulation de la chimie des eaux en milieu argileux pour le projet de stockage de déchets radioactifs en formation géologique. Projet "Archimède argile". European Commission Nuclear Science and Technology. Final report **EUR 17454** FR.

Henrion, P.N., Monsecour, M., Fonteyne, A., Put, M., De Regge, P. 1985. Migration of radionuclides in Boom Clay. *Radioactive waste management and the nuclear fuel cycle* **6**, 313-359.

Jedwab, J., Nicaise, D. 1989. Etude des constituants mineurs de l'Argile de Boom. Unpublished report, 14p.

Laenen, B. 1997. "The geochemical signature of relative sea-level cycles recognised in the Boom Clay". Ph.D. thesis. K.U.Leuven, Leuven, Belgium.

Laenen, B., Hertogen, J., Vandenberghe, N. 1997. The variation of the trace-element content of fossil biogenic apatite through eustatic sea-level cycles. *Palaeogeography, Palaeoclimatology, Palaeocology* **132**, 325-342.

Laenen, B. 1999. The geochemical signature of relative sea-level cycles recognised in the Boom Clay. *Aardkundige mededelingen* **9**, 61-82.

Langmuir, D. 1997. "Aqueous environmental geochemistry". Prentice Hall, New Jersey.

Maes, A., Bruggeman, C., Van Geet M., Deniau, I., Largeau, C. 2003. TRANCOM II, Migration Case Study: Transport of Radionuclides in a Reducing Clay Sediment, Topical report on: Methodologies developed to identify the source of mobile Boom Clay Organic Matter. SCK•CEN report, **BLG-967**, Mol, Belgium.

Marechal, R., Laga, P. 1988. Voorstel lithostratigrafische indeling van het paleogeen. Nationale commissies voor stratigrafie, comissie tertiair, Geologische Dienst, Brussel.

Moors H., Wang L., Vandervoort F., De Cannière P. and Dierckx A. (2002) Assessment of the *in situ* pH and Eh of Boom Clay. *In* "abstracts of Clays in natural and engineered barriers for radioactive waste confinement". International meeting, Reims, France, December 9-12, 2002.

Safir 2 (2001) Safety Assessment and Feasibility Interim Report 2. **NIROND 2001-05 E**.

Stevenson, F.J. 1982. "Humus Chemistry. Genesis, composition, reactions". John Wiley & Sons, New York.

Stumm, W., Morgan, J.J. 1996. "Aquatic Chemistry, 3rd ed.", John Wiley & Sons, New York.

Thorez, J. 1976. Rapport d'analyse mineralogique: contenu qualitatif et semi-quantitatif en mineraux argileux dans l'argile de Boom, au site de Mol (CEN). Intern report, 325/07/030 MiUL.

Van Echelpoel, E. 1991. "Kwantitatieve cyclostratigrafie van de formatie van Boom (Rupeliaan, België). Ph.D. thesis. K.U.Leuven, Leuven, Belgium.

Van Keer, I., De Craen, M. 2001. Sedimentology and diagenetic evolution of the Boom Clay: State of the art. SCK•CEN report, **R-3483**, Mol, Belgium.

Vandenberghe, N. 1978. Sedimentology of the Boom Clay (Rupelian) in Belgium. Verhandeling Koninklijke Academie voor Wetenschappen, Letteren en Schone Kunsten van België, Klasse derWetenschappen, jaargang XL, Nr 147.

Vandenberghe, N., Thorez, J. 1985. XRD-onderzoek van de 14 Å componenten in de kleimineralenfractie van de Boomse klei in de boring te Mol 31W-237. Internal document, Belgian Geological Survey, 7p.

Vandenberghe, N., Van Echelpoel, E. 1987. Field guide to the Rupelian stratotype. *Bulletin de la Société belge de Géologie* **96/4**, 325-337.

Vandenberghe, N. 2003. Rupel Group. *In* "Symposium on the Paleogene, preparing for modern life and climate" (S. Geets, M. Maréchal, P. Laga, M. De Ceuckelaire, S. Gouwy). August 25-30, 2003, Leuven, Belgium.

Van Geet, M. 2002. Interpretation of Rock-Eval data on samples of core HADES 2001/4. Topical report in the frame of D.S. 2.82, Characterisation of Boom Clay organic matter: mobile and immobile fraction. SCK•CEN report, **R-3605**, Mol, Belgium.

Van Geet, M., Maes, N., Dierckx, A. 2003. Characteristics of Boom Clay organic matter, a review. Professional paper, 2003/1, N. 298. Geological Survey of Belgium, Brussels, Belgium, 23p.

Wang, L., Dierckx, A., De Cannière, P. 2000. Speciation and solubility of radionuclides in Boom Clay. Calculations performed with *The Geochemist's Workbench*®-3.1 Database LLNL's version 8 , release 6. SCK•CEN report, **R-3508**, Mol, Belgium.

Wemaere I., Marivoet J., Labat S., Beaufays R. and Maes T. (2002) Mol-1 borehole (April-May 1997), Core manipulations and determination of hydraulic conductivities in the laboratory, annexes 1 to 4. SCK•CEN report, **R-3590A**, Mol, Belgium.

Wouters, L., Vandenberghe, N. 1994. Geologie de la Campine, essai de synthèse. ONDRAF, **NIROND – 94 -12**, Bruxelles (Belgium).

Wouters, L., Herron, M., Abeels, V., Hagood, M., Strobel, J. 1999. Innovative applications of dual range Fourier transform infrared spectroscopy to analysis of Boom Clay mineralogy. *Aardkundige mededelingen* **9**, 159-168.

Zimmerle, W. 1993. On the lithology and provenance of the rupelian Boom Clay in northern Belgium, a volcaniclastic deposit. *Bulletin de la Société belge de Géologie* **102/1-2**, 91-103.

Zimmerle, W. 1998. Petrography of the Boom Clay from the Rupelian type locality, northern Belgium. *In*: "Shales and Mudstones II. Petrography, Petrophysics, Geochemistry, and Economic Geology" (Schieber, Zimmerle and Sethi, Eds), pp. 13-33. Stuttgart.